



HAL
open science

Structural and Functional Insights into the Ligand-binding Domain of a Nonduplicated Retinoid X Nuclear Receptor from the Invertebrate Chordate Amphioxus.

Giuseppe D. Tocchini-Valentini, Natacha Rochel, Hector Escriva, Pierre Germain, Carole Peluso-Iltis, Mathilde Paris, Sarah Sanglier-Cianferani, Alain van Dorsselaer, Dino Moras, Vincent Laudet

► **To cite this version:**

Giuseppe D. Tocchini-Valentini, Natacha Rochel, Hector Escriva, Pierre Germain, Carole Peluso-Iltis, et al.. Structural and Functional Insights into the Ligand-binding Domain of a Nonduplicated Retinoid X Nuclear Receptor from the Invertebrate Chordate Amphioxus.. *Journal of Biological Chemistry*, 2009, 284 (3), pp.1938-1948. 10.1074/jbc.M805692200 . inserm-00357461

HAL Id: inserm-00357461

<https://inserm.hal.science/inserm-00357461>

Submitted on 30 May 2020

HAL is a multi-disciplinary open access archive for the deposit and dissemination of scientific research documents, whether they are published or not. The documents may come from teaching and research institutions in France or abroad, or from public or private research centers.

L'archive ouverte pluridisciplinaire **HAL**, est destinée au dépôt et à la diffusion de documents scientifiques de niveau recherche, publiés ou non, émanant des établissements d'enseignement et de recherche français ou étrangers, des laboratoires publics ou privés.

Copyright

Structural and Functional Insights into the Ligand-binding Domain of a Nonduplicated Retinoid X Nuclear Receptor from the Invertebrate Chordate Amphioxus^{*[5]}

Received for publication, July 24, 2008, and in revised form, October 17, 2008. Published, JBC Papers in Press, November 4, 2008, DOI 10.1074/jbc.M805692200

Giuseppe D. Tocchini-Valentini^{†1,2}, Natacha Rochel^{†1}, Hector Escriva^{§3}, Pierre Germain^{¶1}, Carole Peluso-Iltis[‡], Mathilde Paris[§], Sarah Sanglier-Cianferani^{||}, Alain Van Dorsselaer^{||}, Dino Moras^{‡4}, and Vincent Laudet^{§5}

From the [†]Département de Biologie et de Génomique Structurales and [¶]Département Biologie du Cancer, Institut de Génétique et de Biologie Moléculaire et Cellulaire, UMR7104 CNRS, U596 INSERM, Université Louis Pasteur, 67400 Illkirch, France, [§]Institut de Génomique Fonctionnelle de Lyon, Ecole Normale Supérieure de Lyon, Université Lyon 1, CNRS, INRA, Institut Fédératif 128 Biosciences Gerland, 69364 Lyon Sud, France, and ^{||}Laboratoire de Spectrométrie de Masse Bio-Organique, UMR/CNRS 7178, Institut Pluridisciplinaire Hubert CURIE, Université Louis Pasteur, Ecole de Chimie, Polymères et Matériaux, 67087 Strasbourg, France

Retinoid X nuclear receptors (RXRs), as well as their insect orthologue, ultraspiracle protein (USP), play an important role in the transcription regulation mediated by the nuclear receptors as the common partner of many other nuclear receptors. Phylogenetic and structural studies have shown that the several evolutionary shifts have modified the ligand binding ability of RXRs. To understand the vertebrate-specific character of RXRs, we have studied the RXR ligand-binding domain of the cephalochordate amphioxus (*Branchiostoma floridae*), an invertebrate chordate that predates the genome duplication that produced the three vertebrates RXRs (α , β , and γ). Here we report the crystal structure of a novel apotetramer conformation of the AmphiRXR ligand-binding domain, which shows some similarity with the structures of the arthropods RXR/USPs. AmphiRXR adopts an apo antagonist conformation with a peculiar conformation of helix H11 filling the binding pocket. In contrast to the arthropods RXR/USPs, which cannot be activated by any RXR ligands, our functional data show that AmphiRXR, like the vertebrates/mollusk RXRs, is able to bind and be activated by RXR ligands but less efficiently than

vertebrate RXRs. Our data suggest that amphioxus RXR is, functionally, an intermediate between arthropods RXR/USPs and vertebrate RXRs.

The nuclear receptor (NR)⁶ superfamily is specific to animals and performs an abundance of functions, from embryonic development to metamorphosis and from homeostasis of various physiological functions to the control of metabolism (for a review, see Ref. 1). Nuclear receptors are ligand-activated transcription factors. Many members of the superfamily thus bind major hormones, such as steroids, thyroid hormones, or retinoids. These occupy a special position in gene regulation by providing a direct link between the ligand, which they bind, and the target gene, whose expression they regulate. There are also many nuclear receptors that are not known to bind any ligand and are thus called “orphan nuclear receptors” (2–4). Some nuclear receptors which were originally discovered as orphans have since been shown to bind small hydrophobic molecules, such as fatty acids, but others appear to be true orphans (4).

Nuclear receptors are composed of several functional domains. The N-terminal A/B domain is highly variable in length and sequence and contains a constitutively active transactivation function AF-1. Most conserved are domains C and E, corresponding grossly to the DNA-binding domain and the ligand-binding domain (LBD), respectively. The LBD contains the ligand-dependent transactivation function AF-2. The DNA-binding domain and LBD are connected via a flexible hinge (domain D). NRs act *in vivo* and *in vitro* as ligand-dependent transcriptional transregulators through binding, most often as heterodimers, to *cis*-acting response elements present in cognate target genes. Activation of gene transcription occurs after binding of ligand, which results in a conformational change of the LBD, leading to release of corepressor and binding of coactivator to the LBD (5).

⁶The abbreviations used are: NR, nuclear receptor; RXR, retinoid X nuclear receptor; AmphiRXR, amphioxus RXR; HsRXR, *Homo sapiens* RXR; MmRXR, *Mus musculus* RXR; Bg, RXR, *B. glabrata* RXR; LBD, ligand-binding domain; LBP, ligand-binding pocket; USP, ultraspiracle protein; BtUSP, *B. tabaci*; TcUSP, *T. castaneum* USP; Hx, helix x; RA, retinoic acid; DHA, docohexanoic acid; ESI, electrospray ionization; MS, mass spectrometry.

* This study was supported by CNRS, INSERM, Université Louis Pasteur, European Commission on Structural Proteomics in Europe (SPINE) Grant QL2-CT-220-0098, and SPINE2-Complexes Grant LSHG-CT-2006-031220 under the integrated program, Quality of Life and Management of Living Resources. The costs of publication of this article were defrayed in part by the payment of page charges. This article must therefore be hereby marked “advertisement” in accordance with 18 U.S.C. Section 1734 solely to indicate this fact.

[5] The on-line version of this article (available at <http://www.jbc.org/>) contains supplemental Table 1 and Figs. 1 and 2.

¹ Both of these authors contributed equally to this work.

² Present address: Istituto di Biologia Cellulare, Consiglio Nazionale delle Ricerche, Campus A, Buzzati-Traverso, Via Ramarini 32, Monterotondo Scalo, 00016 Rome, Italy and Istituto di Genetica Molecolare, Consiglio Nazionale delle Ricerche, Via Abbiategrasso 207, I-27100 Pavia, Italy.

³ Present address: Laboratoire Arago, UMR 7628, CNRS and University Pierre and Marie Curie, BP 44, F-66651 Banyuls sur Mer, France.

⁴ To whom correspondence may be addressed: Laboratoire de Biologie et Génomique Structurales, IGBMC, 1 Rue Laurent Fries, BP 10142, Illkirch 67404, France. Tel.: 33-388-653-220; Fax: 33-388-653-276; E-mail: moras@igbmc.u-strasbg.fr.

⁵ To whom correspondence may be addressed: Institut de Génomique Fonctionnelle de Lyon, Molecular Zoology team, Ecole Normale Supérieure de Lyon 1, Institut Fédératif 128 Biosciences Gerland, 69364 Lyon Sud, France. Tel.: 33-472-728-190; Fax: 33-472-728-080; E-mail: vincent.laudet@ens-lyon.fr.

To date, the crystal structures of ~40 different NR LBDs have been solved, mainly mammalian nuclear receptors. All structures are very similar, sharing a common fold containing 11–12 helices (6–7). The majority of the LBD crystals were obtained in the presence of a ligand (holo-LBD) and only a few without ligand (apo-LBD). Comparison of apo- and holo-LBD structures led to the so-called “mouse trap model” of the ligand-dependent conformational switch (8). In apo-LBD, different positions of the C-terminal helix 12 (H12; also called AF-2 helix) highlight the large flexibility of this region (7, 9). In holo-LBD, H12 is folded back on the core of the LBD, closing the LBP. This holo-position of H12 is stabilized by direct or indirect interactions with the ligand. The tightened position of H12, together with H3 and H4, results in the formation of a hydrophobic groove in which coactivator proteins can bind through a conserved LXXLL motif, forming an α -helix. The ligand-induced conformational change concomitantly leads to destruction of the surface that binds the corepressor, resulting in its release from the LBD.

The conserved domains present in NRs allow relatively easy identification of nuclear receptors in genomic sequences (10) and also robust phylogenetic reconstruction on the scale of the superfamily (11, 12). Such analysis shows that NRs for similar ligands do not group in the tree but are interspersed with receptors for totally different ligands, whereas orphans are widely distributed in the tree. This observation has led to the proposal that the superfamily evolved from an orphan receptor that gained the capacity of ligand binding several times independently (13–15). The case of retinoid receptors is interesting in that respect. Indeed, at least two distinct types of nuclear receptors, the RARs (α (NR1B1), β (NR1B2), and γ (NR1B3); activated by all-*trans*-retinoic acid (RA)) and the RXRs (α (NR2B1), β (NR2B2) and γ (NR2B3); activated by 9-*cis*-RA) apparently transduce the retinoid message (16–18). It has thus been proposed that the capacity to bind, for example, retinoic acids, would have been acquired several times by mutation of an orphan nuclear receptor, allowing the establishment of nuclear retinoic acid signaling pathways (RARs and RXRs). The case of RXR and USP, its arthropod homologue, is especially interesting in that context, because this receptor plays a pivotal role inside the NR superfamily as a ubiquitous heterodimer partner for class II NRs (19).

It is noteworthy that structural analysis can provide more insight into the evolution of a protein domain (e.g. through the comparative structural analysis of domains from animals located at critical positions in the evolutionary tree). In that respect, the study of RXR LBD is important, since RXR is an ancient gene that was subjected to several functional shifts during evolution. In addition, the status of RXR as a *bona fide* liganded receptor and the identity of its endogenous ligand are still under discussion (18, 20). Several experiments suggest that there is a very small amount of 9-*cis*-RA *in vivo*, casting doubts on its physiological relevance as an RXR ligand (21). In addition, it has been suggested, from *in vivo* detection of RXR-activating molecules, that docohexanoic acid (DHA) could be a ligand for RXR (22). Thus, it may be possible that 9-*cis*-RA is only a pharmacological activator of RXR.

A large number of homologues of RXR have been identified in a variety of animals including early metazoans, such as sponges and cnidarians, but also arthropods, mollusks, and invertebrate chordates. In cnidarians, RXR was shown to bind 9-*cis*-RA (23), and it activates transcription⁷ in response to it. In contrast, in insects, the orthologue of RXR, called USP, is unable to bind 9-*cis*-RA and experienced a very high evolutionary rate in dipterans and lepidopterans (see Ref. 24 and references therein). Detailed comparative structural analysis of USPs from insects have shown that these can be separated into two different types of receptors: (i) in basal insects, such as hemipterans and coleopterans, the USP ligand-binding pocket is partly filled by residues of unfolded H6 and H11 helices and is thus likely to be an orphan receptor; (ii) in mecopterida (a terminal group of insects that includes dipteras and lepidopteras among others), a phospholipid is present as a structural ligand inside the LBD that may be indicative of the existence of an endogenous ligand yet to be identified (28). In mollusks, RXR can be activated by 9-*cis*-RA and DHA, at least using transient transfection experiments (25). The case of amphioxus is especially interesting, since this species is clearly located in the lineage giving rise to vertebrates but before the complete genome duplications of vertebrates (26) (see Fig. 7 for a phylogenetic tree). Thus, Amphioxus RXR is closely related to the three vertebrate RXR genes but represents a nonduplicated version of these genes. Consequently, determining the structure of the LBD encoded by the unique amphioxus Amphioxus RXR gene and the comparison of this structure with its vertebrate orthologues will infer the main structural features of RXR in the common ancestor of vertebrates (*i.e.* before gene duplication events).

In this paper, we report the crystal structure of the apo form Amphioxus RXR LBD, revealing a stable antagonist conformation not driven by either a fortuitous or an antagonist ligand. A detailed analysis of the comparison with previous crystal structures of HsRXR (29–34), of nonvertebrate RXR (25) and USPs (27, 28) in different conformational states allows us to better understand the evolution and functional dynamics of these orphan receptors and to identify the structural basis of their functional differences.

EXPERIMENTAL PROCEDURES

Cloning and Purification—The cDNA coding for the *Branchiostoma floridae* RXR (accession number AF378829), Amphioxus RXR (35) ligand-binding domain (residues 266–484) was PCR-amplified from pSG5 vector and cloned by homologous recombination into the vector pET15b. The residue's position number given here corresponds to the Amphioxus sequence with the corresponding human sequence numbers within parentheses, (HsAA-xxx), for some residues. The recombinant protein was overproduced and purified in two steps. Briefly, the LBD of Amphioxus RXR (residues 266–484) was cloned in pET15b expression vector to obtain an N-terminal hexahistidine-tagged fusion protein and was overproduced in *Escherichia coli* BL21 (DE3). Cells were grown in LB medium and subsequently induced for 6 h at 20 °C with 1 mM isopropyl thio- β -D-galactoside. Protein purification included a metal

⁷ H. Escriva and V. Lauder, unpublished results.

Amphioxus RXR LBD Structure

affinity chromatography step on a nickel-Hitrap column and a gel filtration on Superdex 75 16/60. The cell pellets were resuspended in binding buffer (20 mM Tris-HCl, pH 8.0, 300 mM NaCl, 10% glycerol, 5 mM imidazole), lysed by sonication, and clarified by centrifugation. The cleared supernatant was loaded on a nickel-Hitrap column (GE Healthcare). The protein was eluted using 150 and 300 mM imidazole, pH 8.0. The protein was subjected to gel filtration on a Superdex 75 16/60 column (GE Healthcare) in 20 mM Tris, pH 8, 200 mM NaCl, and 5 mM dithiothreitol. The protein was then concentrated to 10 mg/ml using a 10K Centricon device. The purity and homogeneity of the protein were assessed by SDS-PAGE and native PAGE and electrospray ionization mass spectrometry. The protein is in equilibrium between homotetramer and homodimer according to analytical gel filtration and native PAGE. The homodimer dissociates into a monomer when characterized by mass spectrometry studies in 50 mM ammonium acetate.

Transient Transfection Assays—293T cells were maintained in Dulbecco's modified Eagle's medium supplemented with 5% of charcoal-treated fetal calf serum. The cells were transfected at 70% confluence in 24-well plates using 4 μ l of ExGen 500 (Euromedex) with 1.0 μ g of total DNA, including 0.1 μ g of reporter plasmid (17m)x5-tk-luc, and 10 ng of cytomegalovirus- β -galactosidase as an internal control to account for variations of transfection efficiency. The culture medium was changed 6 h after transfection, and when appropriate, ligands dissolved in EtOH were added to different final concentrations (10^{-9} to 10^{-6} M). Cells were lysed 24 h after transfection and assayed for luciferase activity. For the test of TIF2 (transcriptional intermediary factor 2) action, 10–500 ng of TIF2 expression vector were assessed.

Pull-down Assays—DNAs of TIF2.1 and TIF2.1m123, kindly provided by Hinrich Gronemeyer (36), were both transcribed and translated *in vitro* using the TNT T7-coupled reticulocyte lysate system (Promega) following the instructions of the manufacturer. Batches of 50 μ M Ni²⁺-nitrilotriacetic acid-agarose gel (Qiagen) washed and equilibrated in buffer A (50 mM Tris-HCl (pH 8.0), 100 mM NaCl, 10 mM MgCl₂, 5 mM imidazole, 10% glycerol, and 0.1% Nonidet P-40) were loaded with 2 μ g of *E. coli*-purified His-tagged LBDs (HsRXR α or Amphioxus). Incubation with TIF2.1 or TIF2.1m123 was done in a final volume of 50 μ l of buffer A containing 2 μ l of *in vitro* translated protein and 10 μ g of bovine serum albumin and in the presence of 2 μ M ligand or 1% of ethanol. After incubation for 1 h at 4 °C and three washing steps in buffer A, bound proteins were recovered with SDS sample buffer and revealed by autoradiography of 12% SDS-polyacrylamide gels.

Electrospray Ionization Mass Spectrometry—Before mass analysis, amphioxus and human RXR LBDs purification buffers were exchanged against 50 mM ammonium acetate on two successive gel filtration columns (NAP-10; GE Healthcare) and then concentrated on Centricon 10-kDa devices. ESI-MS measurements were performed on an electrospray time-of-flight mass spectrometer (LCT; Waters, Manchester, UK). The mass measurements of the noncovalent complexes were performed in ammonium acetate (50 mM, pH 6.8). Samples were diluted to 20 μ M and continuously infused into the ESI ion source at a flow rate of 6 μ l/min through a Harvard syringe pump. Titration

experiments were done by adding 2.5 mol eq of ligands to HsRXR or Amphioxus, followed by a 15-min incubation at 4 °C. Competition experiments were performed by adding an equimolar mixture of two ligands (each in a 2.5-fold molar excess) to the protein, followed by a 15-min incubation. A 2.5-fold molar excess of ligand was used as a standard in our mass spectrometry experiments for two reasons: (i) to be able to detect ligands even with poor affinities (50–100 μ M) and (ii) to assess the specificity of the binding (with a 2.5-fold molar excess, nonspecific binding would also lead to the appearance of bis-adducts, which could not be seen with only a 1:1 ratio). The ligands tested were synthetic (BMS649 and CD3254) or natural (DHA, 9-*cis*-RA, and oleic acid) agonist ligands of HsRXR. 9-*cis*-RA, all-*trans*-RA, oleic acid, and DHA were diluted in 10 mM EtOH. BMS649 and CD3254 were diluted in 10 mM EtOH/DMSO (90:10, v/v). To prevent dissociation in the gas phase during the ionization and desorption process, the cone voltage was optimized to 5 V. Mass data were acquired in the positive ion mode on the *m/z* 1000–5000 mass range. Calibration of the instrument was performed using the multiply charged ions produced by a separate injection of horse heart myoglobin diluted to 2 μ M in 1:1 water/acetonitrile (v/v) acidified with 1% (v/v) formic acid. The relative abundance of the different species present on ESI mass spectra were measured from their respective peak heights (37). All experiments were reproduced at least three times.

An important feature concerning the noncovalent MS approach is whether ESI mass spectra obtained in nondenaturing conditions in the gas phase of the mass spectrometer faithfully reflect direct in solution binding. Several control experiments were performed in order to argue in favor of structurally specific interactions. A series of “successive in solution competitions” strongly argue in favor of site-specific interactions. Instead of the simultaneous addition of a mixture of two ligands, as realized in the direct in solution competitions, successive ligand addition was achieved; a first ligand, L1, is bound to the protein (formation of a 1:1 RXR·L1 complex), and a second one, L2, serves to displace the equilibrium toward the formation of the RXR·L2 complex. Such experiments allow us to unambiguously assess that both ligands compete for the same binding site and that ESI-MS-observed interactions do not result from any artifactual gas phase aggregation. Finally, experiments with different binding partners (either different ligands or human *versus* amphioxus proteins) were also performed, leading to subsequent changes on ESI mass spectra.

Structure Determination—The homodimeric protein fractions were used for crystallization trials. The purified protein conditioned in 20 mM Tris, pH 8.0, 200 mM NaCl, 5 mM dithiothreitol and concentrated to 5 mg/ml. Crystals were grown by the hanging drop diffusion method and appeared in 4 days at 17 °C. The initial drop contained 5 mg/ml protein, 1.5 M sodium acetate, 50 mM *N*-(2-acetamido)iminodiacetic acid, pH 6.5, and was equilibrated *versus* a reservoir containing 1.8 M sodium acetate, 100 mM *N*-(2-acetamido)iminodiacetic acid, pH 6.5. Two different crystals forms, hexagonal and orthorhombic, were obtained in the same crystallization conditions. Only the orthorhombic form resulted in being suitable for structural determination. The solvent content of the crystals is 52.2% with

two LBD dimers (homotetramer) per asymmetric unit. Thus, the homodimeric protein may reassociate with time and salt concentration of the precipitant agent. Crystals were flash cooled in ethane after cryoprotection in a solution containing the reservoir solution plus 25% glycerol. A 2.7 Å resolution data set was obtained merging high and low resolution data sets from only one crystal at the BM29 Synchrotron line of the European Synchrotron Radiation Facility facility in Grenoble. Data were integrated and scaled using the DENZO-SCALEPACK package (38). The program CNS-SOLVE was used throughout the structure determination and refinement calculations (39). An initial phase estimate was obtained by molecular replacement using a partial structure of HsRXR dimer. After a rigid body refinement, the solution resulted in R_{cryst} of 34% and R_{free} of 35%. The model obtained was used to determine the NCS matrix of the four monomer molecules in the asymmetric unit in order to include averaging and solvent flattening procedure of density modification to calculate a first electron density map. The map unequivocally showed the missing parts of the model and allowed the complete manual building of the structure. The phase bias of the initial model was reduced by torsion angle molecular dynamics simulated annealing refinement. Subsequent refinement cycles alternated least square minimization and model building using the program O (40). The NCS was constrained in the first round of refinement and subsequently restrained and released. *B* factors were refined using two groups per residue. In the last cycle, 27 water molecules were located from a difference Fourier map. The loop between H1 and H3 (residues 281–289) and the lateral chains of the residues at positions 271–274, 299, 478, and 482–484 could not be constructed because of poor electron density. The quality of the final model quality was assessed with Procheck. Because of the absence of electron density for the loop between H1 and H3, the integrity of the protein in the crystals was checked by SDS-PAGE (data not shown). For the structure comparison, $C\alpha$ traces of the models were superimposed using the *lsq* commands of O and default parameters. The figures were generated with Pymol. Crystallographic data and refinement statistics are summarized in supplemental Table 1. The chemical structures of all of the ligands described in this paper are shown in supplemental Fig. 1.

RESULTS

Residues That Contact 9-*cis*-Retinoic Acid Are All Conserved between Amphioxus and HsRXR—Previous phylogenetical analysis clearly shows that, as expected, the amphioxus RXR sequence is positioned before the duplications giving rise to the three vertebrate genes (35) (supplemental Fig. 2). In addition, amphioxus RXR was shown to heterodimerize with amphioxus retinoic acid nuclear receptor or thyroid nuclear receptor and to bind to the relevant direct repeat sequence (41, 42).

To determine the crystal structure of the ligand-binding domain we selected a region that encompasses residues 266–484, leaving out the last 30 amino acid of the molecule that form an F-domain with no sequence identity with other NRs. Fig. 1 represents the structure-based sequence alignment of RXR LBDs from different organisms. The alignment reveals a high degree of sequence identity except for the length and composi-

tion of the loop between H1 and H3. Based on the structure of human RXR α , the residues that contact the 9-*cis*-RA are all conserved. The ability to bind this ligand seems thus to be preserved, and this is supported by mass spectrometry studies as well as by transient transfection assays (see below). The same degree of conservation is encountered also in the residues that form the hydrophobic groove in contact with the LXXLL motif activator helix (43). The only exception is a Val residue that in amphioxus RXR substitutes at position 306 a Phe, forming Van der Waals contacts with the coactivator helix. The amino acids of the dimerization interface are strictly conserved (19).

Amphioxus RXR Is Activated by 9-*cis*-RA in Cultured Cells but at Higher Concentrations than Vertebrate RXRs—Since the main residues implicated in ligand binding are conserved between Amphioxus and vertebrates RXRs, we tested whether 9-*cis*-RA and DHA were able to activate Amphioxus RXR in transient transfection assays in mammalian cells. To avoid any interference with endogenous RXR expressed in 293T cells, we used fusions between the Gal4 DNA-binding domain and RXR-LBD. As shown in Fig. 2A, both 9-*cis*-RA and all-*trans*-RA activate 2–4-fold Gal4-MmRXR α and Gal4-Amphioxus RXR. The effect of all-*trans*-RA at the concentration we used can be explained by its isomerization in 9-*cis*-RA (46). Nevertheless, in the experimental condition we used, we did not observe any reproducible effect of DHA (lanes 4 and 8). Of note, using strictly the same conditions as those described in the original paper (22), we observed that DHA activates MmRXR α but not Amphioxus RXR (not shown). Dose response experiments (Fig. 2B) show that 9-*cis*-RA activates Amphioxus RXR in a dose-dependent manner but with a range of concentration higher than mouse RXR. A weak activation by 9-*cis*-RA is also observed for the mollusk *Biomphalaria glabrata* RXR (45). Given that amphioxus is located at the base of chordates in phylogenetical tree, we can conclude from these data that the ability of RXR to bind and to be activated by 9-*cis*-RA is thus conserved in all chordates. This is in accordance with the conservation in amphioxus RXR of the amino acid residues implicated in ligand binding in vertebrate RXRs.

We thus explored the interaction between RXR and coactivators, such as TIF2. The activity of both Gal4-MmRXR α and Gal4-Amphioxus RXR was potentiated by the cotransfection of a human TIF2 expression vector (Fig. 2B). These findings were confirmed by pull-down assays (Fig. 2C) showing that *in vitro* amphioxus RXR, like human RXR α , can interact with TIF2 in a ligand-dependent manner. Interestingly, specific rexinoids, such as BMS649, induce the recruitment of TIF2, but not its mutant TIF2.1m123, mutated in the domain known to interact with NRs. Rexinoids are ligands that selectively bind and activate RXRs but not RARs in contrast to retinoids. This is in accordance with our observation that the recently sequenced amphioxus genome contains a unique homologue of the p160 co-activators (51). All of these observations suggest that (i) the mechanisms by which RXR activates transcription are conserved between amphioxus and mammals and (ii) the binding interface between Amphioxus RXR and TIF2 is functionally conserved.

Amphioxus RXR LBD Structure

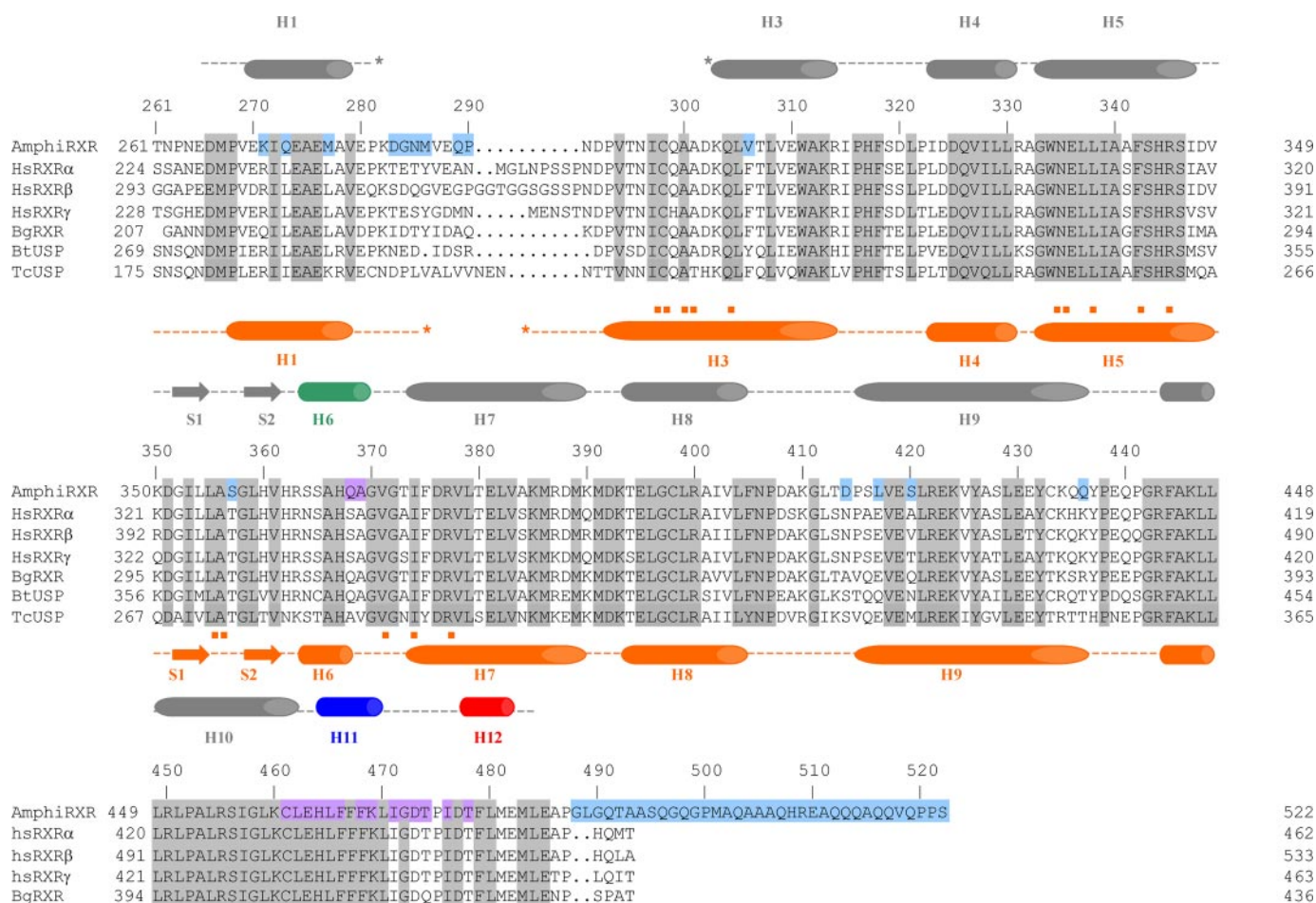


FIGURE 1. Structure-based sequence alignment of the LBD domain of Amphioxus RXR. The sequence of the AmphiRXR LBD is compared with those of human RXR α , RXR β , and RXR γ as well as the USP from *B. tabaci*, *B. glabatra*, and *T. castaneum*. The residues in the blue box are unique to AmphiRXR. The secondary structure of the AmphiRXR and that of 9-*cis*-RA HsRXR α are reported on the top (in gray) and bottom (in orange) lines, respectively. Helix 6, helix 11, and loop 11–12 and helix 12 of AmphiRXR are shown in green, blue, and red, respectively. The residues forming the pocket in HsRXR α are indicated by the orange dots. The residues of AmphiRXR involved in the tetramer interface are shown in purple.

AmphiRXR Binds Retinoid Ligands *In Vitro*—To complement transfection assays, direct evidence for ligand binding to AmphiRXR was given by ESI-MS performed in nondenaturing conditions. Indeed, this particular MS application has proven its efficiency for the characterization of protein-ligand complexes in general and NR LBDs-ligand complexes especially (46–49). No fortuitous ligand was copurified with AmphiRXR. In order to evaluate relative affinities of 9-*cis*-RA, DHA, BMS649, oleic acid, and CD3254 (supplemental Fig. 1) for AmphiRXR LBD in solution titration and competition experiments were monitored by ESI-MS. After fine tuning of the instrumental set-up (see “Experimental Procedures”) in order to avoid dissociation of weak/hydrophobic AmphiRXR/ligand assemblies, titration experiments involving increasing ligand concentrations revealed that all previously mentioned molecules bind to AmphiRXR LBD. Fig. 3 depicts the ESI mass spectra obtained after the addition of a 2.5-fold molar excess (50 μ M) of oleic acid (*B*) 9-*cis*-RA (*C*) or BMS649 (*D*) to AmphiRXR LBD (20 μ M). Peak heights of the different species observed on the ESI mass spectra were considered in order to evaluate relative bound/free protein ratios (37) (see Fig. 3E). In strictly identical experimental and instrumental conditions, only 30% of the AmphiRXR-9-*cis*-RA complexes were detected, whereas up to

80% of the AmphiRXR-ligand complexes were observed for BMS649 and CD3254. Increasing the incubation time from 15 min to 24 h does not change the relative abundances. In the presence of all-*trans*-RA, no ligand binding was observed (data not shown). These results indicate that the synthetic retinoids CD3254 and BMS649 have higher affinities for AmphiRXR than 9-*cis*-RA or oleic acid or DHA, and a relative affinity ranking can be deduced (Fig. 3E). For comparison, similar experiments were performed with HsRXR α LBD, leading always to higher bound/free protein ratios (Fig. 3E). The fact that 9-*cis*-RA presents a higher affinity than DHA for HsRXR α is in agreement with the observations of Lengqvist *et al.* (48, 50). Affinity rankings established by titration experiments for both RXR homologues were further confirmed by direct in solution competition experiments involving a mixture of equimolar amounts of ligands (10 μ M each) and 10 μ M RXR (data not shown). Altogether, these data demonstrate that retinoid ligands that bind to HsRXR also bind to AmphiRXR but with a lower affinity, which is also a proof of the plasticity of the ligand binding property during evolution. The weakest ESI-MS-derived affinity for the tested ligands for AmphiRXR corresponds also to the weakest activation observed in *in vitro* activity assays, which suggests that those ligands are not the natural

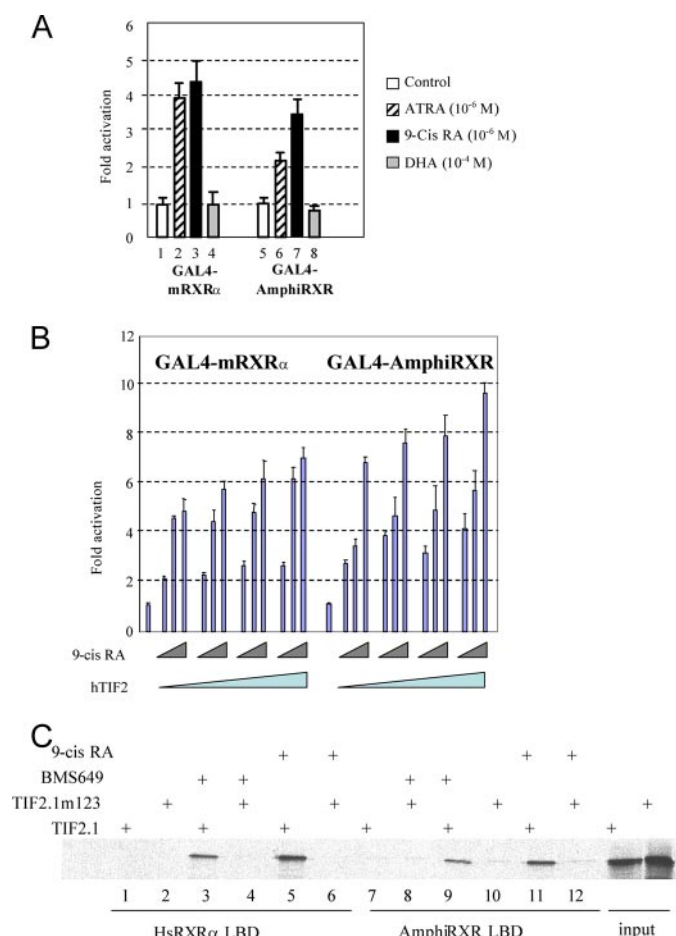


FIGURE 2. Amphioxus RXR is activated by 9-cis-RA in cultured cells. *A*, cells were transfected with Gal4-MmRXR α or Gal4-AmphiRXR along with 17m5-tk-luc reporter plasmid and induced with ligands. *B*, cells were cotransfected with Gal4-MmRXR α or Gal4-AmphiRXR and increasing amounts of hTIF2 (10, 100, 250, and 500 ng), along with the 17m5-tk-luc reporter plasmid, and induced with increasing amounts of ligands (10^{-9} , 10^{-8} , and 10^{-7} M for MmRXR α ; 10^{-9} , 10^{-7} , and 10^{-6} M for AmphiRXR). *C*, purified His-HsRXR α or His-AmphiRXR was incubated in the presence of $2 \mu\text{M}$ BMS649 or $2 \mu\text{M}$ 9-cis-RA and with *in vitro* translated [^{35}S]methionine TIF2.1 or TIF2.1m123, as indicated. Input corresponds to 100% of the TIF2 used in the assays.

ligand, if any, for AmphiRXR. No explanation of the difference in the affinity between amphioxus and human RXR can be found by looking at the residues forming the ligand-binding pocket.

Oligomeric Structure—The asymmetric unit contains two dimers related by a nearly perfect noncrystallographic 2-fold axis (Fig. 4). Within each dimer, the classical dimerization interface (Fig. 4B) is identical to that observed in homodimeric structures of the apo- and holo-HsRXRs (29–34) or USPs (27, 28). It involves helix 10 and, to a lesser extent, helix 9 and the loop between helices 7 and 8 of each monomer. The buried surface of each monomer is 1162 \AA^2 in comparison with 1147 \AA^2 for HsRXR. The tetramer is stabilized by a bottom to bottom organization of dimers reminiscent of the previously reported crystal structures of unliganded RXR (32) but without the intermolecular exchange of helices 12. In the apo-HsRXR (32) and in the apo ascidian RXR tetramer (Protein Data Bank code 2Q60), in addition to the canonical dimer interface, the tetramer interface involves interaction between H3-H3, H11-H11, and H12

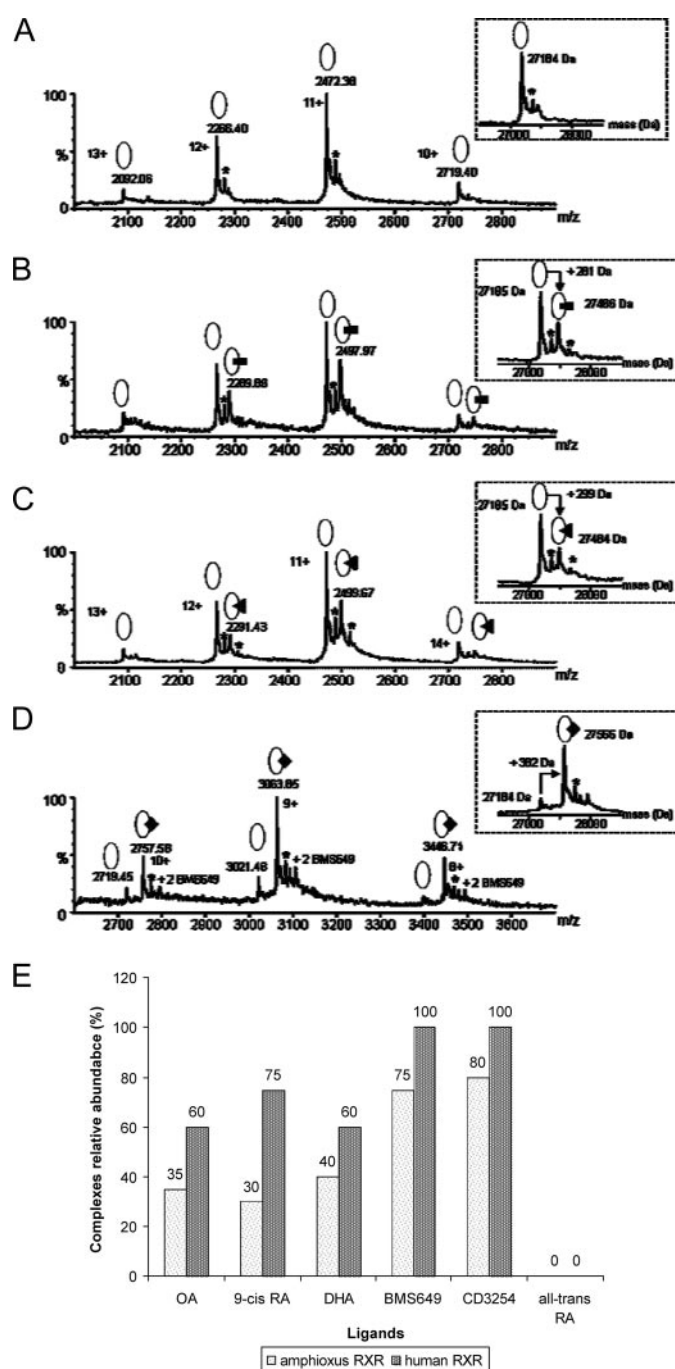


FIGURE 3. Amphioxus RXR LBD binds retinoid ligands. ESI mass spectra of Amphioxus RXR LBD protein (*A*) apo and after incubation with a 2.5-fold molar excess of oleic acid (*B*), of 9-cis-RA (*C*), and of BMS649 (*D*). Deconvoluted mass spectra are presented for each ligand as an inset. *E*, distribution plot of the relative proportion of bound/free protein for AmphiRXR and HsRXR α . Specific binding of both ligands to AmphiRXR is observed with higher affinities for the synthetic ligands CD3254 and BMS649.

that protrudes from one monomer into the coactivator binding site of an adjacent monomer. In the holo-tetramer structure of the mollusk BgRXR (25), within each dimer, one monomer is in open conformation and one is in a closed holo conformation. The open monomers show a swapping of H12 as observed in the apo-HsRXR tetramer, and additional tetramer interfaces are formed between H11 of each closed monomer and H6 of the open monomer in the adjacent canonical dimer (32). In

Amphioxus RXR LBD Structure

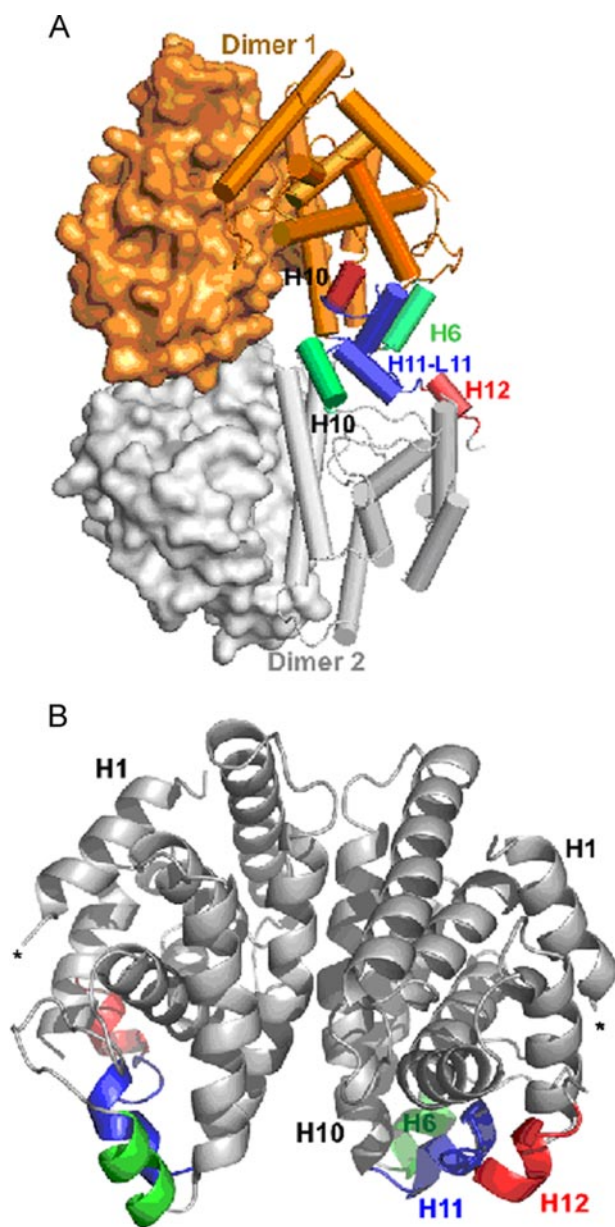


FIGURE 4. Structure of the Amphioxus RXR LBDs. *A*, structure of the tetramer with one dimer shown in orange and the other one in gray. Within each canonical dimer, one monomer is shown in a surface representation, and in the other one, the helices and the β -sheet are represented by cylinders and arrows, respectively. Helix 6 is shown in green, helix 11 and loop 11–12 are in blue, and helix 12 is in red. The same color code is used in all figures. *B*, the Amphioxus RXR homodimer H12 (red) is positioned in the coactivator binding cleft. The missing loop connecting H1 to H3 not visible in the electron density map is shown by stars.

Amphioxus RXR tetramer, the tetrameric interface formed between the two dimers is constituted by residues spanning between helix 10 and helix 12 of one dimer interacting with residues H11 and of H6 of the other. This interface involves mainly Van der Waals contacts and one hydrogen bond between Asp-473 and Lys-468 in the loop H11-H12 of another monomer (Fig. 4). It buries 653 Å² of the surface of each monomer, in contrast to 1215 Å² per monomer for HsRXR, suggesting that the tetramer might actually not be very stable in solution.

Amphioxus RXR Is in an Inactive Conformation—Interestingly, the LBD of Amphioxus RXR exhibits an antagonist-like conforma-

tion with a distorted H12 bound in the coactivator groove. Mass spectrometry showed that Amphioxus RXR does not copurify with any bound ligand. The crystal structure confirms this result, showing no density for a putative small molecule bound. The LBP, as observed in holo-HsRXR, is filled with the partially unfolded H11 (Fig. 5*B*). As a consequence of the conformation of H11, the N-terminal part of H3 is released from its contact to H11. This relaxed structure results in a more flexible H1-H3 connection that translates in a local disorder and explains the absence of clear density for this connection.

Comparison with Mammalian RXRs—The superimposition of the crystal structures of apo- and holo-HsRXR α and Amphioxus RXR LBDs (Fig. 5, *A* and *B*) highlights the unfolding and the reposition of H11 that occupies most of the LBP. In apo-HsRXR α , H11 results from a kink at position 434 (HsGlu-434 in HsRXR α) inducing an 80° twist of the C terminus with respect to the H10 helical axis. As a consequence of this movement, HsLeu-441, HsPhe-437, and HsPhe-438 fill the fraction of the LBP cavity normally occupied by the β -ionone ring of the 9-*cis*-RA ligand (30). In the case of Amphioxus RXR, H11 is partially unfolded and occupies a larger section of the same pocket (Figs. 5*B* and 6). The main differences between the two structures are a consequence of the new position of the shorter H11, which in Amphioxus RXR begins at position Glu-463 (HsGlu-434). The first 6 or 7 residues are not too far in space and present similar orientations of their side chains with Phe-466, Phe-467, Leu-470, and Ile-471, pointing toward the inside core of the protein (Fig. 5). In Amphioxus RXR, Leu-470 carbonyl forms a hydrogen bond with Gln-304 at the C terminus of H3. The Ile-471 side chain contacts Gln-304 and H5. These interactions are stabilized by a network of hydrogen bonds involving main chain carbonyl and amino groups in a pseudohelical conformation (Leu-465–Phe-468, Phe-466–Lys-469, and Phe-467–Leu-470). The C-terminal ends of H11 and H12 have lost their helical conformation to reach the coactivator binding cleft between H3 and H4. As a result, the stabilizing interaction formed with the N-terminal part of H3 disappears. The first 10 residues of H3 and the connection H1-H3 are not visible in the electron density map. This could be the consequence of a static disorder in the crystal, due to a higher flexibility of these fragments and/or a partial unfolding of H3.

A comparison with the holo form of HsRXR α bound to 9-*cis*-RA (Fig. 5*B*) underlines some conformational changes that may be associated with an eventual ligand binding. In the liganded HsRXR α , five residues of H5 contact the ligand; all of these residues are conserved in Amphioxus RXR. Three of these residues keep the same conformation in the absence of the ligand (Asn-335 (HsAsn-306), Leu-338 (HsLeu-309), and Phe-342 (HsPhe-313)) when Trp-334 (HsTrp-305) and Arg-345 (HsArg-316) point in the opposite direction with respect to the pocket (Fig. 6). Arg-345 (HsArg-316) that in holo-HsRXR α forms ionic interactions with the carboxylate group of ligands now points to the solvent. The repositioned lateral chain of Trp-334 is part of a network of interactions that involves Ile-471 of H11, Asp-473 peptidic chain, and Thr-474. These two side chains would easily reorient toward the “bound ligand” pocket.

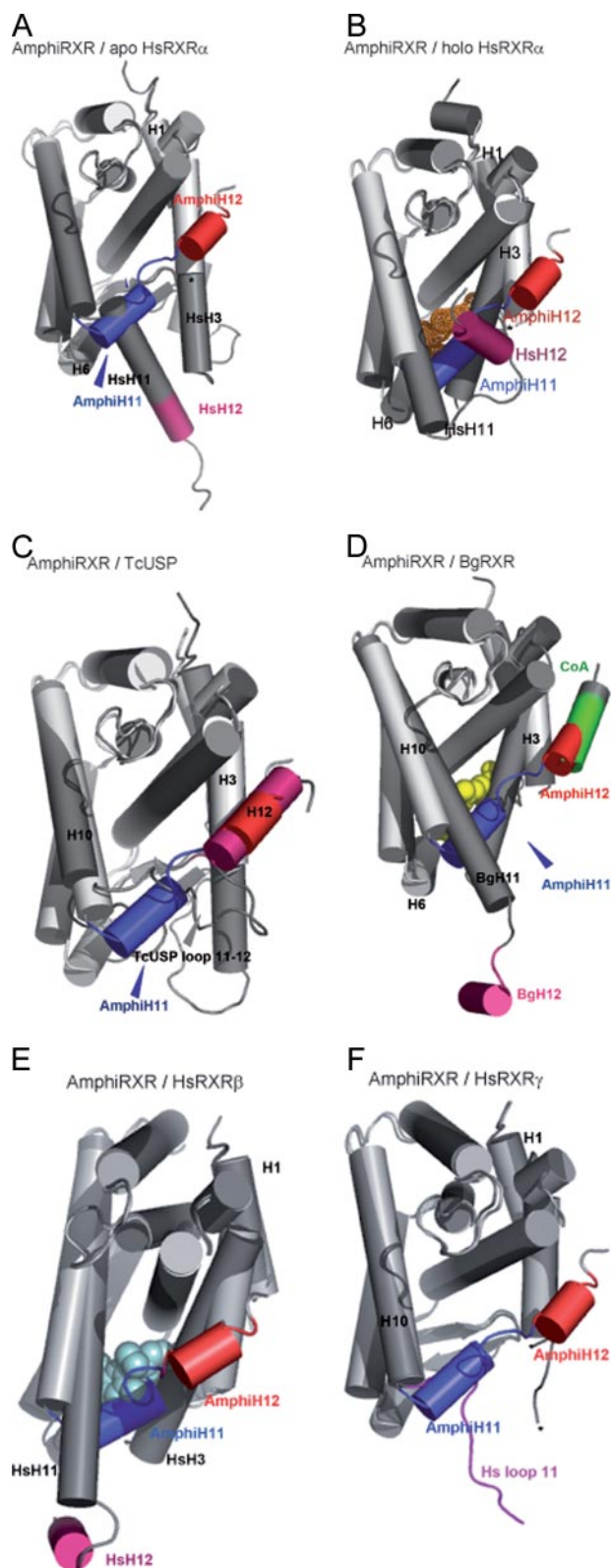


FIGURE 5. Stable apo antagonist conformation of Amphioxus RXR. Shown is the superimposition of Amphioxus RXR (in gray) over apo-HsRXR α (in dark gray) (A), holo-HsRXR α (in dark gray) (B), and TcUSP (in dark gray) (C), showing the close three-dimensional similarity of Amphioxus RXR and TcUSP, notably the conformations of H11 and H12, the open monomer BgRXR (in dark gray) (D), HsRXR β -LG100268 (Protein Data Bank code 1H9U) (in dark gray) (E), and HsRXR γ (Protein Data Bank code 2GL8) (in dark gray) (F). The missing loop 1–3 of Amphioxus RXR is shown by stars. Helices 11 and 12 of Amphioxus RXR are shown in blue and red, respectively. Helices H12 of HsRXR α , TcUSP, BgRXR, and HsRXR β and

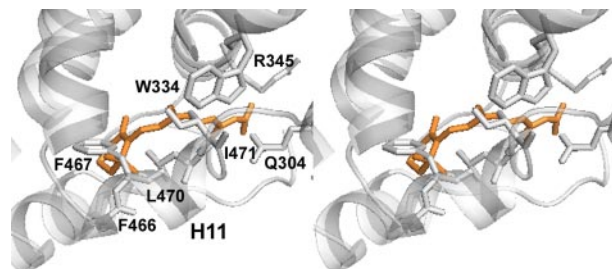


FIGURE 6. Ligand binding cavity of HsRXR α . Shown is a stereoview of the residues filling the AmphiRXR pocket superposed to 9-*cis*-RA (in orange), as observed in the holo-HsRXR α crystal structure.

The two other isoforms of HsRXR have also been crystallized, HsRXR β as a homodimer in complex with the rexinoid LG100268 (33) (Fig. 5E) or a heterodimer with LXR α and in complex with methoprene acid and coactivator peptide (34) and HsRXR γ as an apotetramer (Protein Data Bank code 2GL8) (Fig. 5F). In the homodimer HsRXR β structure, the C-terminal activation helix H12 does not adopt the agonist active conformation and protrudes outside the core of the LBD stabilized by contacts with another dimer in the crystal packing, whereas the rest of the structure is similar to the holo agonist HsRXR α structure. The apo-HsRXR γ tetramer shows an unfolding of H11 and H12 and as a consequence a released N-terminal H3 and absence of density of H1–H3 and the beginning of H3 similar to AmphiRXR. The variability in the position of H12 underlines its flexibility and the lack of a stable “functional” conformation in absence of ligands or cofactors.

Comparison with Invertebrates RXRs—Another invertebrate RXR, the RXR from the mollusk *B. glabrata* has been crystallized in complex with 9-*cis*-retinoic acid and coactivator peptide as a tetramer. In the BgRXR tetramer, within each dimer, one monomer is in open conformation, and one is in a closed holo conformation (25). Both monomers interact similarly with 9-*cis*-RA and coactivator peptide. The open monomers show a swapping of H12, as observed in the apo-HsRXR α tetramer. Although the closed conformation of BgRXR monomer is similar to that of the holo-HsRXR α structure, in the open conformation of BgRXR, the end of H11 and H12 protrudes outside of the core of the LBD despite the presence of ligand and coactivator peptide (Fig. 5C). The main differences between the apo-AmphiRXR structure are the position of the C-terminal H11 and H12 and also the position of H3, which in BgRXR contacts the 9-*cis*-retinoic acid and closes the ligand-binding pocket.

The superimposition of AmphiRXR on USPs from *Bemisia tabaci* (BtUSP) (27) and from *Tribolium castaneum* (TcUSP) (28) emphasizes some striking similarities with these two molecules. In all cases, H11 occupies part of the LBP (Fig. 5D). The main differences concern H6 and H11. In BtUSP and TcUSP, H6 occupies most of the pocket, whereas in AmphiRXR, the LBP is partially occupied by H11. Initially, the absence of H1 and the N terminus of H3 due to proteolysis in BtUSP (27) could provide an explanation for the observed conformational changes of H11 and H12. However, the structure of TcUSP (28)

loop 11–12 of HsRXR γ are colored in pink. The ligands in holo-HsRXR α , -BgRXR, and -HsRXR β are shown by orange surface, and yellow and blue spheres, respectively. The coactivator peptide in BgRXR is shown in green.

Amphioxus RXR LBD Structure

and the present structure clearly establish the functional relevance and the more general character of this apo structure.

DISCUSSION

Although RXR is an early component of the mechanism of regulation of metazoans, the retinoid signaling through RXR is still enigmatic (18, 20). The existence and the necessity of specific endogenous ligands that activate RXR are still controversial (18, 20, 21, 22, 28). Several crystal structures of mammalian RXRs and invertebrate RXRs have revealed an inherent flexibility of H12. Natural retinoid ligands have been shown to be inefficient to reposition H12 in HsRXR β or BgRXR (25, 33, 34). Thus, H12 is only weakly recruited to the canonical active position upon binding of ligands. To learn more about this receptor and to understand the vertebrate-specific character of RXRs, we have studied the RXR ligand-binding domain of the cephalochordate amphioxus, an invertebrate chordate evolutionarily close to vertebrates. Here we report the crystal structure of a novel apotetramer conformation of AmphiRXR LBD. This structure shows some similarities with the crystal structures of the arthropod RXR/USPs that were not observed in mammalian RXR structures. Our functional data demonstrate that AmphiRXR shows weak binding and activation by retinoid ligands. Like the invertebrate BgRXR, AmphiRXR is not activated by retinoids at physiological concentrations. These observations support the proposal of a functional role of this stable apo conformation of AmphiRXR. It is of interest that an AmphiRXR-like conformation is present in insect USPs in functional heterodimers with the ecdysone nuclear receptor (BtEcR/BtUSP and TcEcR/TcUSP) in the agonist conformation and the activation RXR helix in the coactivator binding cleft (antagonist conformation) underlying a silent role of RXR. The capability of AmphiRXR to bind with low affinity retinoids and coactivators, a capability observed for the other invertebrate BgRXR and not observed for TcUSP or BtUSP, may reflect the possibility of a sensor role of the retinoid ligand in the molecular activation of the heterodimeric partner. In that respect, AmphiRXR is similar to BgRXR, and given the current knowledge of the metazoan phylogeny, this may suggest that this corresponds to an ancestral function of RXR (that should be found, for example, in *Tripedalia*) that has been modified in vertebrates and insects (Fig. 7). The role of RXR-specific signaling thus needs to be addressed in further studies. Of note, the amphioxus is a particularly suitable model system for such a study, since it allows treatments with specific agonist or antagonist compounds that will allow dissecting the *in vivo* functional role of this receptor (26). In addition, in amphioxus, several partners of RXR, such as retinoic acid nuclear receptor or thyroid nuclear receptor, have been characterized both in terms of *in vivo* function and in terms of pharmacology (35, 42). Finally the amphioxus genome contains only one gene for each type of receptor (*i.e.* only one RXR, one retinoic acid nuclear receptor, and one thyroid nuclear receptor), thus providing a much simpler system than vertebrates in which genetic redundancy and paralogue-specific sequence divergence impede the understanding of the basal function of a given receptor type (51). Thus, it should be possible using amphioxus to study in more detail the molecular dialogue that may exist between

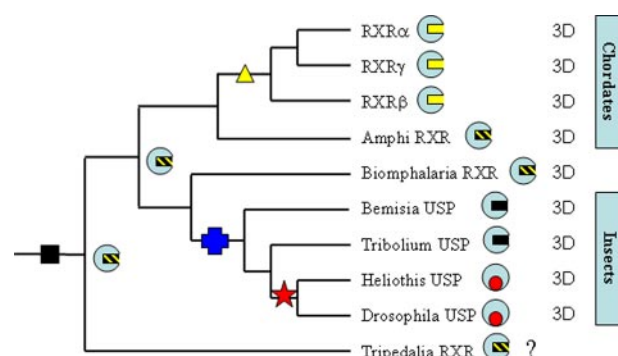


FIGURE 7. Schematized tree of RXRs highlighting the evolutionary and structural plasticity of the ligand-binding domain. Vertebrate RXRs are depicted with an empty binding pocket (yellow) and can readily be activated by low doses of ligands. For AmphiRXR (this study) and mollusk RXR (*Biomphalaria*; see Ref. 25), the ligand-binding pocket is partially filled with H11 residues, but the receptor can still be able to bind a ligand at high doses. A loss of this ligand binding ability occurred at the base of insects (28), giving rise to non-*Mecoptera* USPs (in *Bemisia* and *Tribolium*) that do not bind ligand. A further evolutionary change in *Mecoptera* (*Drosophila* and *Heliothis*) linked to rapid sequence divergence produced receptors exhibiting a large binding pocket filled with a phospholipid. We propose that the situation found in amphioxus and *Biomphalaria* will also be found in cnidarian RXR (*Tripedalia*; see Ref. 23), but this remains to be shown. Colored symbols indicate functional shifts. Black square, early event of gain of ligand binding (15). Blue cross, loss of ligand binding at the base of insects (28) (note that we still ignore precisely when this event occurred). Red star, gain of a structural ligand in *Mecoptera* (28). Yellow triangle, shift of H11 and acquisition of high affinity ligand binding in vertebrates (this study). 3D, the available crystal structure of LBDs.

RXR, its heterodimeric partners, and the transcriptional coactivators.

In this paper, we show that the amphioxus RXR LBD exhibits a striking organization, since it adopts an apo antagonist conformation with a peculiar conformation of helix H11 filling the ligand-binding pocket and shows some similarities with the non-*Mecoptera* insect RXRs in which unfolded H6 and H11 fill the ligand-binding pocket. In addition, our functional data show that AmphiRXR, like the vertebrates and mollusk RXRs, is able to bind and be activated by RXR ligands but less efficiently than vertebrate RXRs. The AmphiRXR LBD is thus structurally similar to the insect USP LBDs, whereas it is functionally related to vertebrate RXRs, since it can be regulated by the same ligands, although with a weaker efficiency. Thus, our data suggest that amphioxus RXR is, functionally, an intermediate between arthropod RXR/USPs and vertebrate RXRs. We propose that in most metazoans, RXR is similar to the situation found in amphioxus or mollusk, and from this situation, two different types of RXR evolved: (i) the ligand-independent form in non-*Mecoptera* insects (further modified later in *Mecoptera*) and (ii) the vertebrate receptors that reinforced their ability to be regulated by ligand binding (yellow star in Fig. 7). Such an event is likely to have occurred before the whole genome duplication events that produced the three paralogous receptors in vertebrates, RXR α , β , and γ , since the three paralogous receptors have identical ligand-binding pockets and exhibit the same ligand binding activities (Fig. 7). Nevertheless, it has to be emphasized that almost no functional data are available from RXRs in nonmammalian vertebrates, such as fishes, or even early vertebrates, such as lamprey and hagfishes. It is only through careful structural and functional analysis of these

receptors that a precise model of ligand binding evolution of chordate RXRs will be determined.

According to the strong conservation of the residues lining the putative canonical LBP, one would predict that all RXR-like LBD, including those from insects, such as the hemipteran *Bemisia* (BtUSP) or the coleopteran *Tribolium* (TcUSP), would bind most of the known ligands of HsRXR. This contrasts with the experimental observations in *Tribolium* USP, which does not bind and is not activated by any RXR ligands (25). Of note, these observations have been reinforced by an evolutionary analysis of the pattern of substitution rate in the ligand-binding domains of RXRs and USPs from a wide variety of metazoans (25). Indeed, these data indicate that in TcUSP or BtUSP, residues that would belong to a potential RXR-like LBP exhibit high evolutionary rates, suggesting a relaxation of the evolutionary pressure in this region that may be related to a loss in ligand binding capability. AmphirXR appears to be in a paradoxical situation when compared with the receptors from insects, since it adopts a similar apo conformation (with H12 in an antagonist position and the ligand-binding pocket filled by H11 residues), whereas it is able to bind to RXR-specific ligands, such as 9-*cis*-retinoic acid, BMS649, or oleic acid. Of note, *in silico* modeling analysis cannot provide a simple steric explanation of this observation, since a homology model that would accommodate ligands like 9-*cis*-RA or fatty acids can easily be built for both the insect receptors and AmphirXR. Additional experiments are necessary to elucidate the mechanism of ligand binding and more generally the question of the necessity of a ligand for this orphan receptor. RXR provides a very clear example showing that sequence conservation is a necessary prerequisite for the prediction of functional properties, such as ligand binding, but is not sufficient alone to reach a conclusion.

Taken together, the data available on RXRs illustrate the remarkable evolutionary plasticity of this LBD that can adapt to different functional shifts, such as changes in the ligand binding abilities, together with a conservation of other functions, such as heterodimerization. This certainly calls for other comparative structural and functional studies of this receptor that will serve to illustrate basic concepts in NR function, such as the role of ligand regulation, the definition of endogenous ligands, or the structural basis of ligand affinity.

REFERENCES

- Gronemeyer, H., Gustafsson, J. A., and Laudet, V. (2004) *Nat. Rev. Drug Discov.* **3**, 950–964
- Gustafsson, J. A. (1999) *Science* **284**, 1285–1286
- Kliwer, S. A., Lehmann, J. M., and Willson, T. M. (1999) *Science* **284**, 757–760
- Benoit, G., Cooney, A., Giguere, V., Ingraham, H., Lazar, M., Muscat, G., Perlmann, T., Renaud, J. P., Schwabe, J., Sladek, F., Tsai, M. J., and Laudet, V. *Pharmacol. Rev.* (2006) **58**, 798–836
- Laudet, V., and Gronemeyer, H. (2002) *The Nuclear Receptor Facts Book*, Academic Press, London
- Wurtz, J. M., Bourguet, W., Renaud, J. P., Vivat, V., Chambon, P., Moras, D., and Gronemeyer, H. (1996) *Nat. Struct. Biol.* **3**, 87–94
- Renaud, J. P., and Moras, D. (2000) *Cell Mol. Life Sci.* **57**, 1748–1769
- Renaud, J. P., Rochel, N., Ruff, M., Vivat, V., Chambon, P., Gronemeyer, H., and Moras, D. (1995) *Nature* **378**, 681–689
- Kallenberger, B. C., Love, J. D., Chatterjee, V. K., and Schwabe, J. W. (2003) *Nat. Struct. Biol.* **10**, 136–140
- Robinson-Rechavi, M., Carpentier, A. S., Duffraisse, M., and Laudet, V. (2001) *Trends Genet.* **17**, 554–556
- Laudet, V., Hänni, C., Coll, J., Catzeflis, F., and Stéhelin, D. (1992) *EMBO J.* **11**, 1003–1013
- Escriva, H., Bertrand, S., and Laudet, V. (2004) *Essays Biochem.* **40**, 11–26
- Escriva, H., Safi, R., Hänni, C., Langlois, M. C., Saumitou-Laprade, P., Stéhelin, D., Capron, A., Pierce, R., and Laudet, V. (1997) *Proc. Natl. Acad. Sci. U. S. A.* **94**, 6803–6808
- Laudet, V. (1997) *J. Mol. Endocrinol.* **19**, 207–226
- Escriva, H., Delaunay, F., and Laudet, V. (2000) *BioEssays* **22**, 717–727
- Germain, P., Staels, B., Dacquet, C., Spedding, M., and Laudet, V. (2006) *Pharmacol. Rev.* **58**, 685–704
- Germain, P., Chambon, P., Eichele, G., Evans, R. M., Lazar, M. A., Leid, M., De Lera, A. R., Lotan, R., Mangelsdorf, D. J., and Gronemeyer, H. (2006) *Pharmacol. Rev.* **58**, 712–725
- Germain, P., Chambon, P., Eichele, G., Evans, R. M., Lazar, M. A., Leid, M., De Lera, A. R., Lotan, R., Mangelsdorf, D. J., and Gronemeyer, H. (2006) *Pharmacol. Rev.* **58**, 760–772
- Brelivet, Y., Kammerer, S., Rochel, N., Poch, O., and Moras, D. (2004) *EMBO Rep.* **5**, 423–429
- Calléja, C., Messaddeq, N., Chapellier, B., Yang, H., Krezel, W., Li, M., Metzger, D., Mascrez, B., Ohta, K., Kagechika, H., Endo, Y., Mark, M., Ghyselinck, N. B., and Chambon, P. (2006) *Genes Dev.* **20**, 1525–1538
- Mic, F. A., Molotkov, A., Benbrook, D. M., and Duester, G. (2003) *Proc. Natl. Acad. Sci. U. S. A.* **100**, 7135–7140
- de Urquiza, A. M., Liu, S., Sjöberg, M., Zetterström, R. H., Griffiths, W., Sjövall, J., and Perlmann, T. (2000) *Science* **290**, 2140–2144
- Kostrouch, Z., Kostrouchova, M., Love, W., Jannini, E., Piatigorsky, J., and Rall, J. E. (1998) *Proc. Natl. Acad. Sci. U. S. A.* **95**, 13442–13447
- Bonneton, F., Zelus, D., Iwema, T., Robinson-Rechavi, M., and Laudet, V. (2003) *Mol. Biol. Evol.* **20**, 541–553
- de Groot, A., de Rosny, E., Juillan-Binard, C., Ferrer, J. L., Laudet, V., Pierce, R. J., Pebay-Peyroula, E., Fontecilla-Camps, J. C., and Borel, F. (2005) *J. Mol. Biol.* **354**, 841–853
- Schubert, M., Escriva, H., Xavier-Neto, J., and Laudet, V. (2006) *Trends Ecol. Evol.* **21**, 269–277
- Carmichael, J. A., Lawrence, M. C., Graham, L. D., Pilling, P. A., Epa, V. C., Noyce, L., Lovrecz, G., Winkler, D. A., Pawlak-Skrzecz, A., Eaton, R. E., Hannan, G. N., and Hill, R. J. (2005) *J. Biol. Chem.* **280**, 22258–22269
- Iwema, T., Billas, I. M., Beck, Y., Bonneton, F., Nierengarten, H., Chaumot, A., Richards, G., Laudet, V., and Moras, D. (2007) *EMBO J.* **26**, 3770–3782
- Bourguet, W., Ruff, M., Chambon, P., Gronemeyer, H., and Moras, D. (1995) *Nature* **375**, 377–382
- Egea, P. F., Mitschler, A., Rochel, N., Ruff, M., Chambon, P., and Moras, D. (2000) *EMBO J.* **19**, 2592–2601
- Bourguet, W., Vivat, V., Wurtz, J. M., Chambon, P., Gronemeyer, H., and Moras, D. (2000) *Mol. Cell.* **5**, 289–298
- Gampe, R. T., Jr., Montana, V. G., Lambert, M. H., Wisely, G. B., Milburn, M. V., and Xu, H. E. (2000) *Genes Dev.* **14**, 2229–2241
- Love, J. D., Gooch, J. T., Benko, S., Li, C., Nagy, L., Chatterjee, V. K., Evans, R. M., and Schwabe, J. W. (2002) *J. Biol. Chem.* **277**, 11385–11391
- Svensson, S., Ostberg, T., Jacobsson, M., Norström, C., Stefansson, K., Hallén, D., Johansson, I. C., Zachrisson, K., Ogg, D., and Jendeborg, L. (2003) *EMBO J.* **22**, 4625–4633
- Escriva, H., Holland, N. D., Gronemeyer, H., Laudet, V., and Holland, L. Z. (2002) *Development* **12**, 2905–2916
- Voegel, J. J., Heine, M. J., Zechel, C., Chambon, P., and Gronemeyer, H. (1996) *EMBO J.* **15**, 3667–3675
- Peschke, M., Verkerk, U. H., and Kebarle, P. (2004) *J. Am. Soc. Mass Spectrom.* **15**, 1424–1434
- Otinowski, Z., and Minor, W. (1997) *Methods Enzymol.* **276**, 307–326
- Brünger, A. T., Adams, P. D., Clore, G. M., DeLano, W. L., Gros, P., Grosse-Kunstleve, R. W., Jiang, J. S., Kuszewski, J., Nilges, M., Pannu, N. S., Read, R. J., Rice, L. M., Simonson, T., and Warren, G. L. (1998) *Acta Crystallogr. Sect. D* **54**, 905–921
- Jones, T. A., Zou, J. Y., Cowan, S. W., and Kjeldgaard, M. (1991) *Acta Crystallogr. Sect. A* **47**, 110–119
- Escriva, H., Bertrand, S., Germain, P., Robinson-Rechavi, M., Umbhauer, M., Cartry, J., Duffraisse, M., Holland, L., Gronemeyer, H., and Laudet, V.

Amphioxus RXR LBD Structure

- (2006) *PLoS Genet.* **2**, e102
42. Paris, M., Escriva, H., Schubert, M., Brunet, F., Brtko, J., Ciesielski, F., Roecklin, D., Vivat-Hannah, V., Jamin, E. L., Cravedi, J. P., Scanlan, T. S., Renaud, J. P., Holland, N. D., and Laudet, V. (2008) *Curr. Biol.* **18**, 825–830
43. Egea, P. F., Mitschler, A., and Moras, D. (2002) *Mol. Endocrinol.* **16**, 987–997
44. Deleted in proof
45. Bouton, D., Escriva, H., de Mendonça, R. L., Glineur, C., Bertin, B., Noël, C., Robinson-Rechavi, M., de Groot, A., Cornette, J., Laudet, V., and Pierce, R. J. (2005) *J. Mol. Endocrinol.* **34**, 567–582
46. Bovet, C., Wortmann, A., Eiler, S., Granger, F., Ruff, M., Gerrits, B., Moras, D., and Zenobi, R. (2007) *Protein Sci.* **16**, 938–946
47. Sanglier, S., Bourguet, W., Germain, P., Chavant, V., Moras, D., Gronemeyer, H., Potier, N., and Van Dorsselaer, A. (2004) *Eur. J. Biochem.* **271**, 4958–4967
48. Lengqvist, J., Mata De Urquiza, A., Bergman, A. C., Willson, T. M., Sjövall, J., Perlmann, T., and Griffiths, W. (2004) *J. Mol. Cell Proteomics* **3**, 692–703
49. Bitsch, F., Aichholz, R., Kallen, J., Geisse, S., Fournier, B., and Schlaeppi, J. M. (2003) *Anal. Biochem.* **323**, 139–149
50. Lengqvist, J., Alvélius, G., Jörnvall, H., Sjövall, J., Perlmann, T., and Griffiths, W. J. (2005) *J. Am. Soc. Mass Spectrom.* **16**, 1631–1640
51. Holland, L. Z., Albalat, R., Azumi, K., Benito-Gutiérrez, E., Blow, M. J., Bronner-Fraser, M., Brunet, F., Butts, T., Candiani, S., Dishaw, L. J., Ferrier, D. E., Garcia-Fernández, J., Gibson-Brown, J. J., Gissi, C., Godzik, A., Hallböök, F., Hirose, D., Hosomichi, K., Ikuta, T., Inoko, H., Kasahara, M., Kasamatsu, J., Kawashima, T., Kimura, A., Kobayashi, M., Kozmik, Z., Kubokawa, K., Laudet, V., Litman, G. W., McHardy, A. C., Meulemans, D., Nonaka, M., Olinski, R. P., Pancer, Z., Pennacchio, L. A., Pestarino, M., Rast, J. P., Rigoutsos, I., Robinson-Rechavi, M., Roch, G., Saiga, H., Sasakura, Y., Satake, M., Satou, Y., Schubert, M., Sherwood, N., Shiina, T., Takatori, N., Tello, J., Vopalensky, P., Wada, S., Xu, A., Ye, Y., Yoshida, K., Yoshizaki, F., Yu, J. K., Zhang, Q., Zmasek, C. M., de Jong, P. J., Osoegawa, K., Putnam, N. H., Rokhsar, D. S., Satoh, N., and Holland, P. W. (2008) *Genome Res.* **18**, 1100–1111

Structural and Functional Insights into the Ligand-binding Domain of a Nonduplicated Retinoid X Nuclear Receptor from the Invertebrate Chordate *Amphioxus*

Giuseppe D. Tocchini-Valentini, Natacha Rochel, Hector Escriva, Pierre Germain, Carole Peluso-Iltis, Mathilde Paris, Sarah Sanglier-Cianferani, Alain Van Dorselaer, Dino Moras and Vincent Laudet

J. Biol. Chem. 2009, 284:1938-1948.

doi: 10.1074/jbc.M805692200 originally published online November 4, 2008

Access the most updated version of this article at doi: [10.1074/jbc.M805692200](https://doi.org/10.1074/jbc.M805692200)

Alerts:

- [When this article is cited](#)
- [When a correction for this article is posted](#)

[Click here](#) to choose from all of JBC's e-mail alerts

Supplemental material:

<http://www.jbc.org/content/suppl/2008/11/06/M805692200.DC1>

This article cites 49 references, 19 of which can be accessed free at

<http://www.jbc.org/content/284/3/1938.full.html#ref-list-1>